JOURNAL OF SOLID STATE CHEMISTRY **133,** 508–515 (1997)
ARTICLE NO. SC977519

# Leucophosphite $K[Fe_2(PO_4)_2(OH)(H_2O)]\cdot H_2O$: Hydrogen Bonding and Structural Relationships

Stefan Dick[1]

*Institut für Anorganische Chemie der Universität München, Meiserstr. 1, 80333 München, Germany*

and

Thomas Zeiske

*Institut für Kristallographie, Universität Tübingen, c/o Hahn-Meitner-Institut, Glienickerstr. 100, 14109 Berlin, Germany*

Received March 31, 1997; in revised form June 18, 1997; accepted June 23, 1997

**Hydrogen atom positions in leucophosphite $K[Fe_2(PO_4)_2(OH)(H_2O)]\cdot H_2O$ were elucidated by Rietveld refinement of a powder neutron scattering diffractogram. Crystal data: $a = 975.6(3)$, $b = 966.4(3)$, $c = 976.9(4)$ pm, $\beta = 102.43(2)^\circ$, $R_{wp} = 0.084$. This experiment proved that the Fe-atoms in the tetrameric $Fe_4O_2$ building units of leucophosphite are bridged by hydroxo groups and that the phosphate tetrahedra are not protonated. While the water molecule O(10) bound to Fe acts only as a H-bond donor, the second water molecule O(11) between the tetrameric units donates and accepts H-bonds. Together with oxygen atoms from phosphate groups a six-membered ring of oxygen atoms, connected by hydrogen bonds, is formed. Water O(11) is held in the structure by comparably weak H-bonds so that it is already lost at 396(3) K. $Fe_4O_2$ tetramers topological analogous to those in leucophosphite are found in the minerals spheniscidite, melonjosephite, and amarantite, and in a number of synthetic iron complexes. The structural relationships of leucophosphite with compounds containing $M_4O_2$ clusters ($M$ = Al, Ga, Mo) are discussed.** 

## INTRODUCTION

Leucophosphite $K[Fe_2(PO_4)_2(OH)(H_2O)]\cdot H_2O$ has been found in nature mainly as a product of mineral alteration by guano deposits (1–3), in pegmatite deposits (4–6), and recently in lateritic crusts (7). Like other aluminum and iron phosphates containing $NH_4$ and K leucophosphite is also formed by the reaction of soil minerals with fertilizers (8–10). A structure determination of leucophosphite from the Tip Top pegmatite was performed by Moore in 1972 (11); it showed that leucophosphite contains tetramers of Fe-centered octahedra linked by phosphate tetrahedra to a three-dimensional framework. A hydrogen bonding scheme was proposed from O ··· O distances and geometrical considerations.

In context with our studies concerning hydrated $M$(I)–$M$(III)–phosphates (13–15) we tried to describe the hydrogen bonding in leucophosphite more exactly. Thus we performed a neutron scattering experiment with synthetic leucophosphite powder. In addition, structural relationships between leucophosphite and analogous compounds with tetrameric building units are described.

## EXPERIMENTAL

### *Synthesis*

Leucophosphite powder was synthesized by the reaction of 4.70 g of synthetic goethite (16) with 500 ml of a 1 $M$ K-phosphate solution of pH 2 at 373 K in a glass beaker under vigorous stirring. After 5 days the product was filtered off, washed phosphate-free with water, and air dried. Leucophosphite powder containing coarser crystals was synthesized by the hydrothermal reaction of freshly prepared $FePO_4\cdot nH_2O$ (1.0 g) with 25 ml 2.5 $M$ K-phosphate solution (pH 2) at 423 K for 14 days in a Teflon-lined autoclave.

### *Powder Neutron Scattering*

A neutron powder diffractogram of synthetic leucophosphite was measured at the Hahn-Meitner-Institut Berlin on the diffractometer E2 (Research Proposal CHE-01-507). The wavelength of $\lambda = 241.71$ pm (pyrographite monochromator) was calibrated against a diffractogram of $\alpha$-Fe and the known lattice constant of that sample. Diffraction data were recorded with a $^{10}BF_3$ multidetector in a $2\theta$ range

[1] To whom correspondence should be addressed.



0022-4596/97 $25.00

from 6.0° to 85.0° until a monitor had accumulated $1.7 \times 10^7$ counts (measuring time approximately 3 h) and were corrected for detector cell efficiency.

Rietveld analysis of the obtained diffractogram was performed with the program PROFIL (18). As a starting model, cell constants and atomic parameters from a redetermination of the leucophosphite structure were used. Background intensities were estimated graphically and modeled by nine background points. After refinement of scale factor, diffractometer shift, cell constants, an asymmetry parameter for Gaussian peak shape, and resolution parameters ($u$, $v$, $w$) $R_{wp}$ had dropped to 0.24. A further decrease of $R_{wp}$ was achieved by additional refinement of positions and isotropic displacement parameters of H-atoms, while all parameters of non-H-atoms were kept fixed. With 28 parameters, refinement converged at $R_{wp} = 0.084$.

### *Thermal Analysis*

Thermal analysis of synthetic leucophosphite powder was performed with a Mettler DSC between 300 and 575 K in a $N_2$ atmosphere. Standard deviations for $\Delta H$ and onset temperatures were determined from five measurements of individual samples.

## RESULTS AND DISCUSSION

### *Synthesis of Leucophosphite*

Goethite as well as freshly prepared $FePO_4 \cdot nH_2O$ can be used as the Fe source for the preparation of leucophosphite. Experiments using goethite and 1 *M* K-phosphate solutions with pH values of 2, 4, and 5.5 at 353 and 373 K indicate that in all cases leucophosphite is formed as the stable compound. While at the lowest pH value crystalline products ($KFe(HPO_4)_2 \cdot H_2O$ and $K_2Fe_2(HPO_4)_2 \cdot H_2O$) occur and finally transform into leucophosphite, at pH 4 and 5.5 amorphous Fe–phosphates are formed which slowly yield crystalline leucophosphite.

These observations may have some importance for the discussion of the genesis of leucophosphite and strengite in nature. In literature (1, 7) it is assumed that leucophosphite is only stable under alkaline conditions and that it transforms to strengite under acidification. Our results, however, suggest that at least in the presence of phosphate in high excess leucophosphate is stable at pH values as low as 2.

### *Structure of Leucophosphite*

The structure model of leucophosphite, as published by Moore (11) and incorporated in the ICSD, contains unreasonable short K–O distances. A redetermination of the structure with a single crystal from Těškov (Bohemia, Czech Republic) yielded very similar cell constants (cf. Table 5) and atomic parameters with a decreased $R$ value ($R_g = 0.054$ for 3191 reflections and 167 refined parameters; details of that structure determination are deposited under CSD-406691 at the Fachinformationszentrum Karlsruhe, 67344 Eggenstein-Leopoldshafen, Germany). Atomic coordinates and displacement parameters for the redetermined leucophosphite structure are listed in Table 1. In fact, a simple misprint of a K parameter in the paper of Moore (11) was the reason for the unacceptable short bond distances (12).

The structure of leucophosphite is best described in terms of $Fe_4O_2$ building units (Fig. 1) that are connected to a three-dimensional framework by phosphate tetrahedra. The $Fe_4O_2$ units are formed by a central pair of edge sharing $FeO_6$ octahedra ($2 \times$ Fe(1) connected via O(9)), to which two additional $FeO_6$ octahedra are attached by corner sharing ($2 \times$ Fe(2) via O(9)). Both types of $FeO_6$ octahedra are distorted and exhibit extraordinary long bonds to O(9). While the four iron atoms lie in one plane, the bridging oxygen atoms O(9) and O(9A) lie 56.6 pm above and below that plane. Each of the two phosphate tetrahedra is connected with two Fe(1) and two Fe(2) octahedra, thus creating a three-dimensional framework of $PO_4$ tetrahedra and the $Fe_4O_2$ units. This framework contains intersecting tunnels running through the structure. Tunnels running along [010] are occupied by K-ions (Fig. 2). Water molecules O(11) are situated between the $Fe_4O_2$ units and connected with the Fe–phosphate framework by hydrogen bonds only.

**TABLE 1**
**Atomic Coordinates ($\times 10^4$) and Equivalent Displacement Coefficients ($pm^2\ 10^{-1}$) for Leucophosphite from Těškov**

| Atom | $x$ | $y$ | $z$ | $U_{eq}$[a] |
|---|---|---|---|---|
| K | 5174(2) | 1956(1) | 8989(1) | 25(1) |
| Fe(1) | 3916(1) | 5508(1) | 3693(1) | 8(1) |
| Fe(2) | 5971(1) | 2278(1) | 3099(1) | 9(1) |
| P(1) | 7911(1) | 287(1) | 1455(1) | 7(1) |
| P(2) | 7896(1) | 1785(1) | 6290(1) | 7(1) |
| O(1) | 9359(3) | 929(3) | 1990(3) | 10(1) |
| O(2) | 6749(4) | 1205(3) | 1758(3) | 11(1) |
| O(3) | 7614(3) | 87(3) | − 152(3) | 9(1) |
| O(4) | 7159(4) | 3861(3) | 2846(3) | 11(1) |
| O(5) | 9410(4) | 2304(4) | 6554(3) | 13(1) |
| O(6) | 7847(4) | 327(3) | 6955(3) | 10(1) |
| O(7) | 6955(4) | 2729(3) | 6944(3) | 12(1) |
| O(8) | 7351(4) | 1632(3) | 4712(3) | 12(1) |
| O(9) | 4969(4) | 3570(3) | 4385(3) | 9(1) |
| O(10) | 4889(4) | 477(4) | 3436(4) | 22(1) |
| O(11) | 3098(6) | 1531(4) | 5331(5) | 28(2) |
| H(9) | 4229(61) | 2872(37) | 4454(50) | 13(6) |
| H(1) | 5315(54) | − 302(46) | 3952(47) | 38(10) |
| H(2) | 3890(40) | 307(57) | 3092(64) | 38(10) |
| H(3) | 2573(58) | 976(55) | 4564(55) | 51(16) |
| H(4) | 2537(54) | 1429(64) | 6104(54) | 51(16) |

*Note.* Parameters of H-atoms were determined by neutron scattering of synthetic material.

[a] $U_{eq}$ is defined as a third of the trace of the orthogonalized $U_{ij}$ tensor.

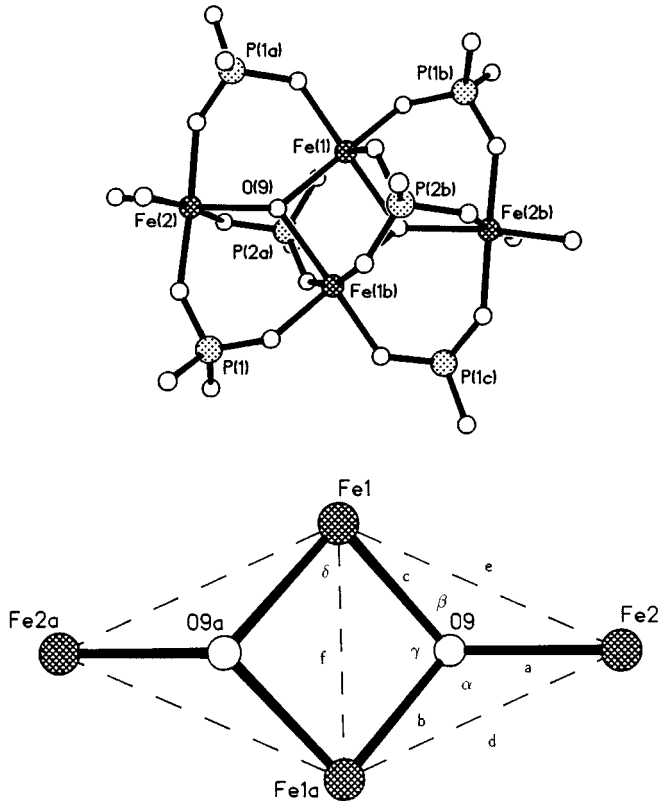


**FIG. 1.** The structure of the $Fe_4$ unit in leucophosphite; top, ball and stick representation with phosphate coordination; bottom, $Fe_4O_2$ core with definitions of characteristic distances and angles.

*Hydrogen Bonding in Leucophosphite*

In order to elucidate the hydrogen positions in leucophosphite a neutron scattering experiment with synthetic leucophosphite powder was performed. A summary of data for this experiment can be found in Table 2. For the Rietveld refinement of the neutron powder pattern of leucophosphite, several models regarding different hydrogen bonding schemes were tested: (i) a hydrogen atom attached to O(9) or not (oxo- or hydroxo-bridges in the $Fe_4O_2$ unit); (ii) two or three hydrogen atoms coordinating O(11) with short bond lengths ($H_2O$ or $H_3O^+$); (iii) hydrogen atoms attached to O(2) and/or O(8), i.e., phosphate or hydrogen phosphate groups around P(1) and/or P(2). In addition, structure models with hydrogen bonds to other oxygen atoms with reasonable distances and models with disordered H sites were tried. The only model that could be refined successfully is very similar to the scheme that had been proposed by Moore from $O \cdots O$ distances and geometrical considerations. The obtained H-atom positions can be found in Table 1, bond distances and angles are summarized in Table 3. Figure 3 shows the Rietveld plot for the neutron powder diffractogram.

According to these results O(9) is certainly protonated so that the iron centers in the $Fe_4O_2$ units are bridged by hydroxo- rather than oxo-groups. Both O(10) and O(11) are oxygen atoms of water molecules with quite normal bond angles (H(1)–O(10)–H(2), 111(4)°; H(3)–O(11)–H(4), 105(4)°). Phosphates P(1) and P(2) are both involved in hydrogen bonding but are phosphate groups and by no means hydrogen phosphate molecules. Regarding their function as hydrogen bond donors and acceptors the building units of leucophosphite form three groups (cf. Fig. 4): (i) the water molecule of O(10) acts as a hydrogen bond donor (via H(1) and H(2)) only; (ii) phosphates P(1) and P(2) only accept hydrogen bonds; (iii) the water molecule of O(11) acts as a donor as well as an acceptor for two H-bonds.

As shown in Fig. 4, O(11), O(10), and O(6) form a centrosymmetric six-membered ring with distorted chair conformation. The bridging hydrogen atoms lie near the $O \cdots O$ vectors and exhibit angles between 153° and 171° to the oxygen atoms. Regarding $O \cdots H$ distances, the hydrogen bonds in leucophosphite seem to be comparably weak. The shortest distance is found between H(2) and O(6), while the longest and probably weakest H-bond is formed by H(9) and O(11).

The hydrogen atoms H(3), H(4), H(9), and H(1) create a distorted tetrahedral coordination of O(11). While the water molecule O(11) acts as an H-bond donor to two phosphate tetrahedra, it accepts two hydrogen bonds from a water molecule O(10) and a hydroxo group O(9). This tetrahedral surrounding of O(11) resembles the coordination of the interlayer water in taranakite (14). Like in taranakite the hydrogen positions seem to be ordered around the tetrahedrally coordinated oxygen, in contrary to the situation in ice $I_h$ (19, 20) were disordered H sites have been found.

*Thermal Behavior*

Between 300 and 575 K two endothermic phase transitions of first order are observed during DSC analysis. The onset temperatures are 396(3) and 453(3) K, respectively. A gravimetric experiment showed that in this temperature range a weight loss of 9.4% occurs, indicating the removal of two water molecules per formula (calc. 9.1%). The first phase transition can be assigned to the loss of water O(11). The reaction enthalpy $\Delta H$ is 33(2) kJ/mol and therefore comparable with the loss of the interlayer water in taranakite ($\Delta H = 33(2)$ kJ/mol), which is also held in the structure by hydrogen bonds only (14). The second reaction at 453 K is accompanied by a considerable change of $c_p$ and can be assigned to the removal of water O(10) and the resulting breakdown of the structure. The larger enthalpy $\Delta H = 47(3)$ kJ/mol reflects the bonding of O(10) to Fe besides the formation of two hydrogen bonds.

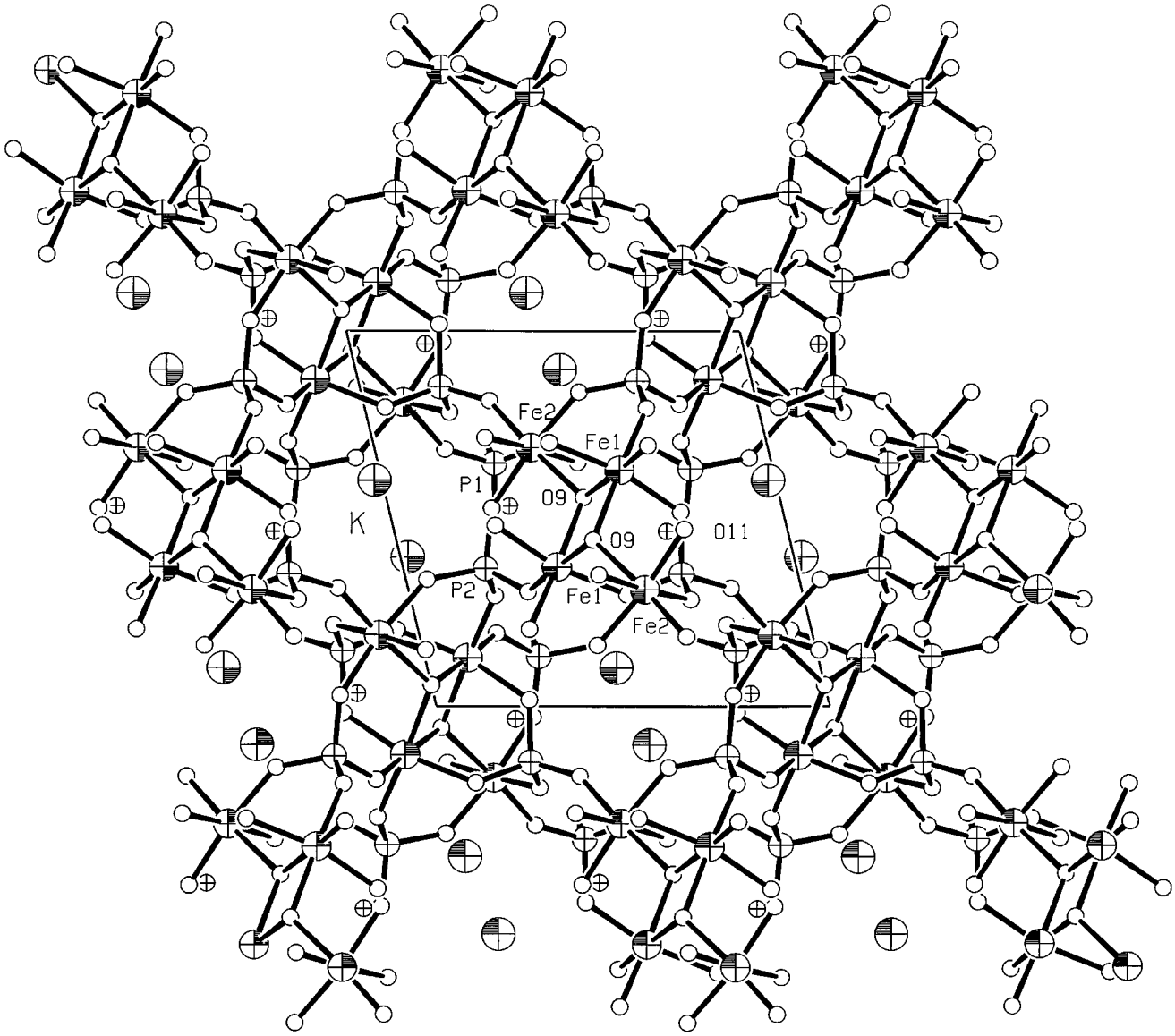


**FIG. 2.** Perspective view of the leucophosphite structure along 010.

*Structural Relationships with Compounds Containing $Fe_4O_2$ Units*

Topological analogues of the $Fe_4O_2$ clusters in leucophosphite occur in the minerals spheniscidite (21) (the $NH_4$ analogue of leucophosphite), melonjosephite $Ca_2[(Fe^{2+}_{0.5}Fe^{3+}_{0.5})_4(OH)_2(PO_4)_4]$ (22), and amarantite $Fe_2(SO_4)_2O\cdot 7H_2O$ (23). In amarantite, however, no hydroxo- but oxo-groups link the Fe octahedra. Comparable oxo-bridged $Fe_4O_2$ cores have been found in the synthetic Fe(III) complexes[2] $[Fe_4O_2(CH_3CO_2)_7(bpy)_2]^{2+}$ (24), $[Fe_4O_2(C_6H_5CO_2)_7(H_2B(pz)_2)_2]^-$ (25), $[Fe_4O_2(CF_3CO_2)_8(H_2O)_6]$ (26), and $[Fe_4O_2(bicoh)_2(bico)_2(C_6H_5CO_2)_4]^{2+}$ (27). The first two complexes show a "bent butterfly" structure of the $Fe_4O_2$ core; in the latter two compounds the ion atoms lie in one plane as in leucophosphite.

From another point of view the $Fe_4O_2$ clusters in leucophosphite can be regarded as dimers of binuclear units Fe(1)–O(9)–Fe(2). This structural feature is found in a lot of iron complexes with various terminal and bridging ligands (e.g., carboxylates and organophosphates), oxidation states of iron and oxo- as well as hydroxo-bridges (28), e.g., in the binuclear hydroxo-bridged Fe(III) complex $[Fe_2(HPTP)(OH)(NO_3)_2]^{2+}$ (29). At last, the $Fe_4O_2$ cluster can also be seen as a derivative of a trinuclear unit to which a fourth

[2] Abbreviations used: bpy = 2,2′-bipyridyl; $H_2B(pz)_2$ = dihydrobis(1-pyrazolyl)borate; bicoh = bis(*N*-methylimidazol-2-yl)carbinol; HPTP = *N*,*N*,*N*′,*N*′-tetrakis(2-pydridylmethyl)-2-hydroxy-1,3-diaminopropane.

**TABLE 2**
**Summary of Data for Powder Neutron Diffraction of Leucoposphite**

| | |
|---|---|
| Formula | $K[Fe_2(PO_4)_2(OH)(H_2O)]\cdot H_2O$ |
| Space group | $P2_1/n$ |
| Lattice constants | $a = 975.6(3)$ pm |
| | $b = 966.4(3)$ pm |
| | $c = 976.9(4)$ pm |
| | $\beta = 102.43(2)^\circ$ |
| $Z$ | 4 |
| $2\theta$ range | 6.0–85.0° |
| $2\theta$ resolution | 0.1° |
| Wavelength | $\lambda = 241.71$ pm |
| No. of data points | 790 |
| No. of reflections | 155 |
| No. of parameters | 28 |
| Peak width parameters ($u/v/w$) | 2.8(4)/ − 1.4(3)/0.41(4) |
| Residuals[a] $R_{exp}/R_I/R_{wp}$ | 0.063/0.077/0.084 |

[a] $R_{exp} = \sqrt{(N-P+C)/\sum w y_{obs}^2}$; $R_I = \sum |I_{obs} - I_{calc}|/\sum I_{obs}$; $R_{wp} = \sqrt{\sum w(y_{obs} - y_{calc})^2/\sum w y_{obs}^2}$, with $y_{total} = y_{total}$ − background and $w = y_{obs}^{-1}$.

**TABLE 3**
**Interatomic Distances and Angles of H Atoms in Leucophosphite as Determined by Powder Neutron Scattering**

| O–H ⋯ O | | | O–H (pm) | O ⋯ H (pm) | Angle O–H ⋯ O (deg) |
|---|---|---|---|---|---|
| O(9) | **H(9)** | O(11) | 100(5) | 202(5) | 160(4) |
| O(10) | **H(1)** | O(11) | 95(4) | 197(4) | 153(4) |
| O(10) | **H(2)** | O(6) | 97(4) | 179(4) | 159(5) |
| O(11) | **H(3)** | O(6) | 97(5) | 192(5) | 162(5) |
| O(11) | **H(4)** | O(4) | 102(5) | 184(5) | 160(4) |

$FeO_6$ octahedron is attached via one edge. The $Fe_3O$ motif of Fe(1), Fe(1A), Fe(2), and O(9) is found in the basic iron carboxylates $[Fe_3O(RCO_3)_6]^+$. The three Fe centers and the bridging oxo-group lie in one plane in the trinuclear complex, leading to a trigonal planar coordination of O.

In Table 4 characteristic geometric data of the minerals and complexes mentioned above are compiled. The interatomic distances and angles are defined as shown in Fig. 1 and chosen according to (24, 27). As this table shows, leucophosphite and spheniscidite are extraordinary members of the $Fe_4O_2$ compounds. The longest Fe–O bonds and, as a consequence, the longest Fe ⋯ Fe distances are found in these minerals. As expected the Fe–O bond lengths increase with protonation of the bridging oxygen. The Fe–O–Fe and O–Fe(1)–O angles are very similar in all $Fe_4O_2$ systems; the nature of the bridging ligands seems to have only a minor influence on this angles. In the tetranuclear systems the Fe(1)–O–Fe(2) angles are between 123° and 137°, and the "inner" Fe(1)–O–Fe(1A) angles are between 90° and 97°. In the case of leucophosphite these angles together with H(9) lead a coordination of the bridging O(9) that lies between a distorted tetrahedral and a distorted trigonal pyramid configuration.

In all compounds the Fe(1) ⋯ Fe(1A) distances are comparably small, especially in the oxo-bridged species. The unusual short distance in amarantite led to the assumption that direct spin coupling of the two edge-sharing iron centers is responsible for the red color of this mineral, in contrast to the pale color of leucophosphite (11). The

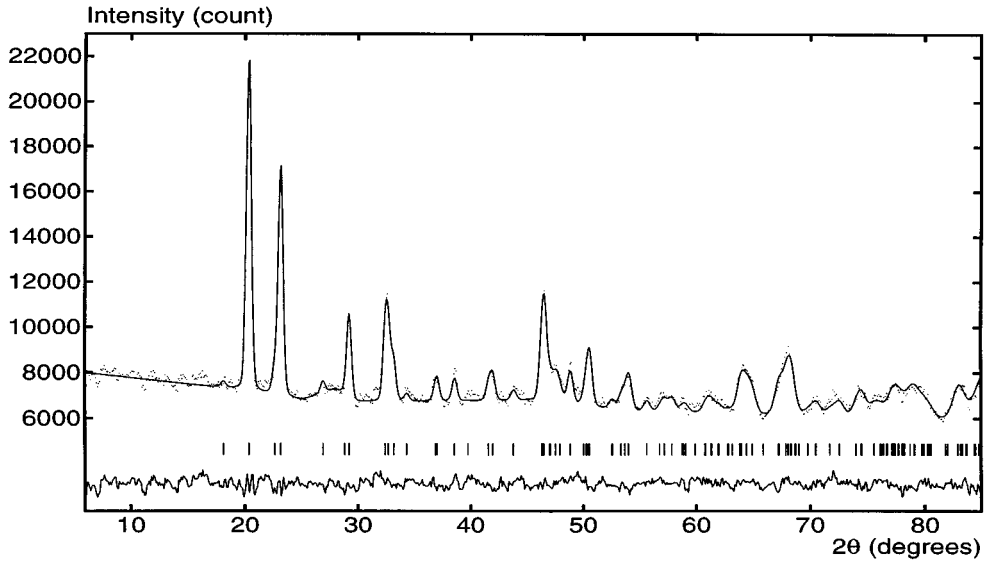


**FIG. 3.** Observed, calculated, and difference profiles for neutron scattering of synthetic leucophosphite powder. Vertical tick marks indicate calculated reflection positions.

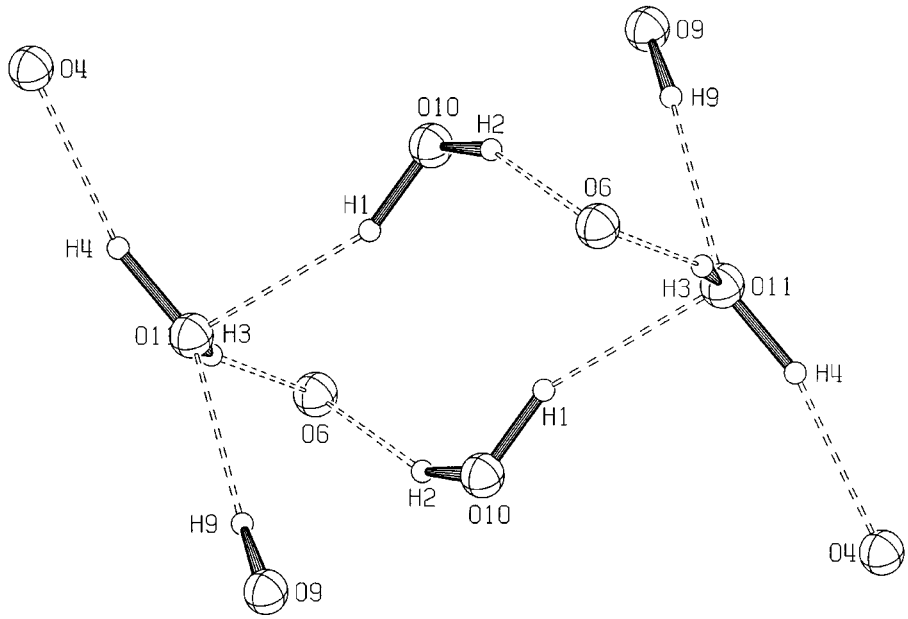


**FIG. 4.** Hydrogen bonding scheme in leucophosphite.

analysis of electronic spectra of oxo- and hydroxo-bridged binuclear Fe(III) complexes suggests that the type of the bridging ligand plays the most important role for the color of these systems. Oxo-bridged complexes show strong absorption bands in the region of 300–400 nm ("oxo dimer region", oxo → Fe CT transitions (28)) while the pale-colored hydroxo-bridged complexes lack that absorption feature. The deep color of melonjosephite may be attributed to the presence of both Fe(II) and Fe(III) in the $Fe_4O_2$ clusters (22).

### *Structural Relationships with Leucophosphite Analogous Compounds*

In the past years a number of leucophosphite analogous compounds with topologically identical $M_4O_2$ units ($M$ = Al, Ga, Mo), very similar cell criteria, and analogous structures have been found (Table 5). Isomorphous substitution in leucophosphite leads to a series of nonstochiometric compounds with formula $[K_{1-x}(NH_4)_x][Fe_{1-y}Al_y(PO_4)_2(OH)(H_2O)]\cdot H_2O$. The members with ideally $x = y = 0$ (leucophosphite), $x = 1$ and $y = 0$ (spheniscidite), $x = 0$ and $y = 1$ (tinsleyite) occur as minerals (32, 30) and have been characterized by structure determination (21, 31). The compound with $x = y = 1$ is formed by the reaction of soil constituents with phosphate fertilizers (33); its structure has been described recently (12, 34). Formal replacement of $Al^{3+}$ by $Ga^{3+}$ and $K^+$ by $H_3O^+$ leads to $(H_3O)[Ga_2(PO_4)_2(OH)(H_2O)]\cdot H_2O$, a hydrated Ga–phosphate $GaPO_4\cdot 2H_2O$ with leucophosphite structure (35). An analogous compound with $NH_4^+$ at the $H_3O^+$ site was found in $(NH_4)[Ga_2(PO_4)_2(OH)(H_2O)]\cdot H_2O$ (37) and $GaPO_4$–$C_7$ (36).

**TABLE 4**
**Characteristic Data for $Fe_4O_2$ Cores in Minerals and Related Synthetic Complexes**

| Compound | a | b | c | d | e | f | α | β | γ | δ |
|---|---|---|---|---|---|---|---|---|---|---|
| Leucophosphite | 215 | 215 | 217 | 382 | 377 | 310 | 123 | 92 | 124 | 88 |
| Spheniscidite | 215 | 216 | 217 | 382 | 379 | 312 | 123 | 92 | 125 | 88 |
| Melonjosephite | 203 | 210 | 210 | 365 | 365 | 297 | 124 | 90 | 124 | 90 |
| Amarantite | 189 | 193 | 197 | 348 | 349 | 290 | 128 | 96 | 132 | 84 |
| $Fe_4O_2$ complexes (min) | 182 | 195 | 190 | 329 | 343 | 283 | 119 | 94 | 129 | 83 |
| $Fe_4O_2$ complexes (max) | 188 | 198 | 196 | 347 | 359 | 294 | 134 | 97 | 137 | 86 |
| $(Fe_2(HPTP)(OH)(NO_3)_2)^{2+}$ | 200 | 199 | | 322 | | | 108 | | | |
| $(Fe_3O(CH_3CO_2)_6)^+$ | 188 | 190 | 191 | 329 | 327 | 329 | 119 | 120 | 121 | |

*Note.* All numbers are rounded to the last digit. Interatomic distances a–f (pm) and angles α–δ (deg) are defined in Fig. 1.

**TABLE 5**
**Comparison of Lattice Constants (pm and deg) of Leucophosphite Analogous Compounds in Space Group $P2_1/n$**

| Compound | Origin | Method[a] | Ref. | *a* | *b* | *c* | *β* |
|---|---|---|---|---|---|---|---|
| Leucophosphite | Tip Top mine | X/s | (11)[b] | 975.1(9) | 965.8(2) | 978.2(9) | 102.24(12) |
| Leucophosphite | Těškov quarry | X/s | This work | 973.6(4) | 964.7(4) | 975.8(4) | 102.50(3) |
| Leucophosphite | Synthetic | N/p | This work | 975.6(3) | 966.4(3) | 976.9(4) | 102.43(2) |
| Tinsleyite | Tip Top mine | X/s | (30)[b] | 954.3(11) | 953.2(6) | 960.2(8) | 103.16(6) |
| Tinsleyite | Synthetic | X/s | (31) | 949.9(2) | 950.3(2) | 953.5(2) | 103.26(3) |
| Spheniscidite | Elephant Island | X/p | (32)[b] | 970(1) | 963(1) | 975(1) | 102.57(12) |
| Spheniscidite | Synthetic | X/s | (21) | 982.32(6) | 973.76(8) | 987.16(8) | 102.803(8) |
| $NH_4Al_2(PO_4)_2(OH)\cdot 2H_2O$ | Synthetic | X/s | (12)[b] | 955.63(3) | 957.20(4) | 961.67(3) | 103.589(2) |
| $NH_4Al_2(PO_4)_2(OH)\cdot 2H_2O$ | Synthetic | X/s | (34) | 955.3(1) | 957.7(1) | 961.4(1) | 103.56(1) |
| $GaPO_4\cdot 2H_2O$ | Synthetic | X/s | (35)[b] | 968(1) | 964(1) | 977(1) | 102.7(2) |
| $GaPO_4$–$C_7$[c] | Synthetic | X/s | (36) | 968.1(3) | 965.7(3) | 976.2(3) | 102.90(2) |
| $NH_4Ga_2(PO_4)_2(OH)\cdot 2H_2O$ | Synthetic | X/s | (37)[b] | 968.9(1) | 970.3(1) | 978.8(1) | 102.80(2) |
| $NH_4Mo_2P_2O_{10}\cdot H_2O$ | Synthetic | X/s | (38) | 978.0(10) | 968.1(5) | 988.4(8) | 102.17(8) |
| $RbMo_2P_2O_{10}\cdot(1-x)H_2O$ | Synthetic | X/s | (39) | 978.6(3) | 976.2(1) | 983.8(2) | 102.04(2) |

[a] X, X ray; N, neutron; s, single crystal; p, powder.
[b] *a*- and *c*-axes were exchanged according to $c > a$.
[c] $GaPO_4$–$C_7 = NH_4Ga_2(PO_4)_2(OH)\cdot 2H_2O\cdot 0.16$ PrOH.

The formation of leucophosphite analogous structures is not restricted to phosphates of main group metals. The structures of $NH_4Mo_2P_2O_{10}\cdot H_2O$ (38) and $RbMo_2P_2O_{10}\cdot(1-x)H_2O$ (39) are analogous but not isotypic with leucophosphite in the strict sense of this term, since they contain oxo-bridged rather than hydroxo-bridged clusters (38, 39). In the latter two compounds the distances between the metal atoms in the central pair of octahedra in the tetranuclear unit (distance *f* in Fig. 1) is small enough to allow for Mo–Mo double bonds in contrary to the Al or Fe compounds. Analogous $Mo_4O_2$ tetramers, besides other building units, have been found in $Cs_2Mo_7O_9(PO_4)_7\cdot H_2O$ (40). At last it should be noted that tetramers of oxo-bridged trigonal bipyramids instead of octahedra were shown to exist in $AlPO_4$–12(en) and $GaPO_4$–12(en) ($Al_3(PO_4)_3\cdot H_2O\cdot$en and $Ga_3(PO_4)_3\cdot H_2O\cdot$en) (41). These compounds also contain channels filled with the organic template molecules.

## ACKNOWLEDGMENTS

We are indebted to Prof. Dr. Dr. h.c. Armin Weiss for support of this work. Financial support of the neutron scattering experiments by the Berlin Neutron Scattering Center (BENSC) is gratefully acknowledged.

## REFERENCES

1. J. M. Axelrod, M. K. Carron, and T. P. Thayer, *Am. Mineral.* **37,** 883 (1952).
2. G. C. Simmons, *Am. Mineral.* **49,** 337 (1964).
3. M. J. Wilson and D. C. Bain, *Am. Mineral.* **61,** 1027 (1976).
4. M. L. Lindberg, *Am. Mineral.* **42,** 214 (1957).
5. R. A. Bhaskara and M. S. Adusumilli, *Mineral. Mag.* **35,** 784 (1966).
6. P. B. Leavens and T. A. Simpson, *Mineral. Rec.* **6,** 66 (1975).
7. H. Tiessen, S. Lo Monaco, A. Ramirez, M. C. D. Santos, and C. Shang, *Biogeochemistry* **34,** 1 (1996).
8. J. F. Haseman, J. R. Lehr, and J. P. Smith, *Soil Sci. Soc. Am. Proc.* **15,** 76 (1951).
9. J. P. Smith and W. E. Brown, *Am. Mineral.* **44,** 138 (1959).
10. W. Lindsay, P. Vlek, and S. Chien, *in* "Minerals in Soil Environments" (J. B. Dixon and S. B. Weed, Eds.), No. 1, p. 1089. SSSA Book Series, Soil Science Society of America, Madison, WI, 1989.
11. P. B. Moore, *Am. Mineral.* **57,** 397 (1972).
12. J. J. Pluth, J. V. Smith, J. M. Bennett, and J. P. Cohen, *Acta Crystallogr. Sect. C* **40,** 2008 (1984).
13. S. Dick, U. Gossner, A. Weiss, G. Grossmann, G. Ohms, and M. Müller, *J. Solid State Chem.* [in press]
14. S. Dick, U. Gossner, A. Weiss, G. Grossmann, G. Ohms, and T. Zeiske, *Inorg. Chim. Acta* [in press].
15. S. Dick and T. Zeiske, *Inorg. Chemistry.* [In preparation]
16. U. Schwertmann, *in* "Iron oxides in the laboratory: Preparation and characterization," pp. 61, VCH, Weinheim, 1991.
17. G. M. Sheldrick, "SHELXTL-Plus Crystallographic System." Siemens Analytical X-Ray Instruments, Madison, WI, 1989.
18. Cockroft, J., "PROFIL—A Rietveld Program." 5.17 (1994).
19. S. W. Peterson and H. I. Levy, *Acta Crystallogr.* **10,** 70 (1957).
20. A. J. Leadbetter, R. C. Ward, J. W. Clark, P. A. Tucker, T. Matsuo, and H. Suga, *J. Chem. Phys.* **82,** 424 (1985).
21. M. Cavellec, D. Riou, and G. Ferey, *Acta Crystallogr. Sect. C* **50,** 1379 (1994).
22. A. R. Kampf and P. B. Moore, *Am. Mineral.* **62,** 60 (1977).
23. P. Süsse, *Z. Kristallogr.* **127,** 261 (1968).
24. J. K. McCusker, J. B. Vincent, E. A. Schmitt, L. M. Mino, K. Shin, D. K. Coggin, P. M. Hagen, J. C. Huffmann, G. Christou, and D. N. Hendrickson, *J. Am. Chem. Soc.* **113,** 3012 (1991).
25. W. A. Armstrong, M. E. Roth, and S. J. Lippard, *J. Am. Chem. Soc.* **109,** 6318 (1987).
26. V. I. Ponomarev, L. O. Atovmyan, S. A. Bobkova, and A. Turte, *Dokl. Akad. Nauk. SSSR* **274,** 368 (1984).
27. S. M. Gorun and S. J. Lippard, *Inorg. Chem.* **27,** 149 (1988).
28. D. Kurtz, *Chem. Rev.* **90,** 585 (1990).

29. A. Weiss and S. Dick, *Z. Naturforsch.* **49b,** 1051 (1994).
30. P. J. Dunn, R. C. Rouse, T. J. Campbell, and W. L. Roberts, *Am. Mineral.* **69,** 374 (1984).
31. S. Dick, *Z. Anorg. Allg. Chem.* [submitted]
32. M. Wilson and D. C. Bain, *Mineral. Mag.* **50,** 291 (1986).
33. E. C. Sample, R. J. Soper, and G. J. Racz, "The role of phosphorus in agriculture" (F. E. Khasawneh et al., Eds.), p. 263. ASA, Madison, WI, 1980.
34. J. B. Parise, *Acta Crystallogr. Sect. C* **40,** 1641 (1984).
35. R. C. L. Mooney-Slater, *Acta Crystallogr.* **20,** 526 (1996).
36. Wang Tieli, Yang Guangdi, Feng Shouhua, Shang Changjjang, and Xu Ruren, *J. Chem. Soc., Chem. Commun.*, 948 (1989).
37. T. Loiseau and G. Ferey, *Eur. J. Solid State Inorg. Chem.*, 575 (1994).
38. H. E. King, L. A. Mundi, K. G. Strohmaier, and R. C. Haushalter, *J. Solid State Chem.* **92,** 1 (1991).
39. A. Leclaire, M. M. Borel, A. Grandin, and B. Raveau, *J. Solid State Chem.* **108,** 177 (1994).
40. A. Guesdon, M. M. Borel, A. Leclaire, A. Grandin, and B. Raveau, *J. Solid State Chem.* **111,** 315 (1994).
41. J. B. Parise, *Inorg. Chem.* **24,** 4312 (1985).